Modeling Zika Virus Transmission Dynamics: Parameter Estimates, Disease Characteristics, and Prevention

Munsur Rahman[1], Kidist Bekele-Maxwell[2], Leanna Cates[3], H.T. Banks[2], Naveen K. Vaidya[4,*]

[1]University of Missouri-Kansas City, Civil & Mechanical Engineering Department, Kansas City, 64110, USA
[2]N.C. State University, Center for Research in Scientific Computation, Raleigh, 27695, USA
[3]Stowers Institute for Medical Research, Kansas City, 64110, USA
[4]University of Missouri-Kansas City, Department of Mathematics and Statistics, Kansas City, 64110, USA
*Corresponding author: vaidyan@umkc.edu

Several outbreaks of the Zika virus (ZIKV), including the 2007 outbreak in Yap Island, the 2013-14 outbreak in French Polynesia, and the recent devastating spread of the virus across the Americas, have posed a public health emergency of international concern. Because of limited data availabilty, much remains uncertain about paramters related to ZIKV dynamics. In this study, we used a mathematical model, thorough fitting procedures, and a recently investigated complex-step derivative approximation technique to properly identify parameters that can be estimated using available epidemic data from French Polynesia and Yap Island. Our analysis showed that the parameters that can be estimated may vary from Island to Island, suggesting that the parameters estimated based on standard techniques may provide misinformation about the ZIKV transmission dynamics. Using our techniques, we carefully estimated ZIKV related parameters and computed basic reproduction numbers ranging from 1.90 to 3.31. Furthermore, we used our model to evaluate potential prevention strategies and found that peak prevalence can be reduced to nearly 10% by reducing mosquito-to-human contact by at least 60% or increasing mosquito death by at least a factor of three. With these levels of prevention programs, the final outbreak size is predicted to be negligible, thereby successfully controlling ZIKV epidemics.

Introduction

The Zika virus (ZIKV) was first isolated in a Ugandan forest from a febrile rhesus monkey in 1947 [1]. The first major outbreaks of ZIKV arose in Yap and Micronesia between April and July 2007 [2], followed by an additional outbreak in French Polynesia between October 2013 and April 2014 [3]. Recently in 2015, ZIKV rose to prominence in American countries, more specifically in Brazil and Colombia [4-6], areas where the epidemic form of ZIKV were previously uncommon. In February 2016, the World Health Organization (WHO) declared ZIKV to be a public health emergency of international concern[7], and the Center for Disease Control (CDC) have set their response efforts to a Level 1 activation, which is the highest response level at the agency[8]. This devastating spread of the virus poses a major global public health emergency and prompts worldwide attention.

ZIKV, a member of the Flavivirade family, is primarily vector-borne, with some reported cases of sexual or blood-fusion transmission [1-3,5]. This arbovirus is spread by the *Aedes* genus of mosquito, which is also the primary vector for other well-known viruses like Dengue, Chikungunya, and yellow fever [2,4,6]. Therefore, ZIKV is likely to flourish in tropical areas similar to the French Polynesian landscape. ZIKV symptoms include fever, myalgia/arthralgia, edema of extremities, maculopapular rash, retro-orbital pain, conjunctivitis, and lymphadenopathies [9]. Growing evidence suggests that ZIKV is linked to several neurological disorders, such as Guillain-Barre Syndrome [10,11] and microcephaly in infants born to mothers who were infected with ZIKV during pregnancy [12,13]. These phenomena have been observed in both epidemics in French Polynesia and South America. Unfortunately, there is no specific treatment of this diseases, and at this moment the illness cannot be prevented by medications or vaccines. Because of the absence of treatment and vaccines, the immediate control strategy of ZIKV will rely on the control of mosquito and/or human-mosquito contacts. It is thus critical to get insights into the transmission dynamics of ZIKV in the population and evaluate potential control strategies.

Mathematical modeling has become a crucial tool in understanding dynamics and designing prevention and control measures for infectious diseases[14-19]. Previous modeling studies on ZIKV have advanced our understanding of the ZIKV infection and related paramteres[2,20,21], but limited experimental and theoretical studies have left much to be desired. In particular, previous studies [2,21] have estimated the parameters from model fitting without considering that all parameters might not be accurately estimated from the limited data sets. Moreover, all data sets might not be useful to accurately estimate the same parameters. The parameter estimation from model fitting without thorough analysis on their confidence may lead to incorrect estimation and may provide misinformation about ZIKV transmission dynamics. Therefore, the key epidemiological parameters, including the basic reproduction number, still remain uncertain and there is a lack of detailed evaluation on potential control strategies. Such studies based on proper parameter estimation and validation could inform future prevention measures, such as outbreak planning or assessment of potential countermeasures, and thereby decrease the potential of the virus to become a pandemic.

In this study, we formulated mathematical models of between-hosts transmission dynamics of ZIKV infection and developed a method to thoroughly analyze the parameters that can be estimated from a given limited data. Importantly, we identified the ZIKV related parameters that can be confidently estimated from the survey data from six islands of French Polynesia and one island of the Federated States of Micronesia (weekly new infected population); the parameters that can be estimated may vary from Island to Island. Using these properly estimated parameters through our model, we computed the basic reproduction number and performed extensive analysis and simulation of the models to study short-term and long-term dynamics of the disease, prevalence of infections, and effect of prevention programs on disease outcomes.

Results

Identification of parameters that can be estimated. We fitted our model to the cumulative new infection data from each of six islands of French Polynesia (Tahiti, Sous-le-vent, Moorea, Tuamotu-Gambier, Marquises, Australes) and Yap island. We first estimated five parameters along with their respective standard errors (Table 1). With these parameters, the model simulations exhibited reasonble agreement with the data (Fig. S-1). However, as we can observe from Table 1, the standard errors for the estimated parameters are very large, giving negative lower limit of 95% confidence interval. The reason for the poor confidence intervals could be that the data may

not be sufficient to estimate all five parameters (this can be seen as only the model solution P is used in the inverse problem to estimate these parameters) and/or the model solution P may not be very sensitive to all five parameters. Estimates with poor confidence intervals may not provide reliable information about the ZIKV dynamics.

To achieve reliable confidence intervals, we compute the standard errors and the sensitivity of P to all five parameters at the estimated values (Fig. 1). As seen in Fig. 1, the magnitude of the sensitivity of P to one of the parameters (mostly η) is bigger in a multiple of magnitudes than each of the rest. In addition, the model solution is sensitive to most of the other parameters only for short period of time. In each case, we identified the least sensitive parameter and fixed it. Then we fitted the model to the data to estimate the remaining four parameters (Table S-1). We repeated the process by increasing the number of fixed parameters one more at a time until each estimated parameter has a reliable confidence interval (Table S-2 and Table S-3). For the data considered here, the standard errors along with sensitivity results suggest that the data sets do not contain sufficient information to estimate more than three parameters in islands of French Polynesia and more than two parameters in Yap island with a reasonable degree of certainty attached to the estimates. Importantly, the parameters that can be estimated differ from island to island. Parameters that can be estimated for each island are given in Table 2.

Best parameter estimates. As discussed above, in each case we cannot estimate all unknown parameters with reasonable confidence intervals from the given data sets. However, our method has identified the parameters that can be estimated for each island. Using this information (Table 2), for each island, the paramters that need to be fixed are taken as the average of the confidently estimated parameters from other islands. Then, with these parameters fixed, we again fitted the model to data from each island. The best parameters obtained for each island along with their 95% confidence intervals are given in Table 2. With these parameters, the model prediction along with the survey data for each island is shown in Fig 2. In addition, we also computed the weekly new infection predicted by the model and compared them with the experimental survey data (Fig. 3). These best parameters estimated with reliable confidence intervals provide excellent agreement with the experimental data from each of the 7 islands considered (Figs. 2, 3).

Characteristics of ZIKV transmission dynamics. Our estimate shows that the mosquito-to-human transmission rate, $\hat{\beta}_h$, is about 0.95 per day for all islands of French Polynesia and 0.91 per day for Yap island (Table 2). Human-to-mosquito transmission rate, β_m, ranges from 0.03 per day in Marquises to 0.11 per day in Moorea. It shows that the per day rates of a human being infected through the mosquito bites are approximately 10 to 30 times more than a mosquito being infected.

Our predicted human incubation $(1/\alpha_h)$ period is about 4 to 12 days and the infectious $(1/\gamma_h)$ period is about 11 to 12 days. These predictions are consistent with some estimated laboratory data [22,23].

Estimated values of η indicate that only small portion of predicted Zika infection was reported to the health sentinel sites. The reported cases ranged from 2.85% in Tahiti to 20.59% in Yap. This shows that an actual epidemic size of the ZIKV could be significantly higher than that seemed in the reported cases. This is in agreement with the fact that individuals infected with ZIKV usually do not show any signs or symptoms and are most likely to be unreported.

Basic reproduction number. The Basic Reproduction Number, R_0, is defined as the average number of secondary cases generated by a typical infectious individual in a fully susceptible population [17]. The disease dies out if $R_0 < 1$ and the epidemic occurs if $R_0 > 1$. We calculated R_0 for our model using the next generation operator approach [24]. We obtained the basic reproduction number for our model as follows:

$$R_0 = \sqrt{\frac{\widehat{\beta}_h \beta_m \alpha_m}{\gamma_h \lambda_m (\alpha_m + \lambda_m)}} \quad (1)$$

.

Using the estimated parameters in equation (6), we obtained the basic reproduction number, R_0, with a value ranging from 1.90 in Marquises to 3.31 in Moorea island (Table 3). The model predicts R_0>1 in each island, and there were ZIKV epidemics, which is consistent with the observations in the data collected.

We further examined the sensitivity of the parameters on the reproduction number R_0 using the normalized forward sensitivity index S_x given by:

$$S_x = \frac{x}{R_0} \frac{\partial \mathrm{R}_0}{\partial \mathrm{x}} \quad (2)$$

where x is one of the parameters whose sensitivity on R_0 is sought. This index implies that the higher the value in its magnitude, the more sensitive the parameter to the value of R_0. Our result shows that the basic reproduction number is more sensitive to mosquito lifespan than any other parameters (Fig. 4), suggesting that prevention programs focused on reducing mosquito lifespan can be more effective for avoiding ZIKV infection. Such measurements can be useful to identify and quantify the effective prevention strategies.

Disease outcomes: prevalence and outbreak size. Our model predicts the mean prevalence of infection across all islands to be at its peak between the initial 8 to 10 weeks of infection. The amplitude of the peak suggests that during peak time of infection 30-35% of the total population will be affected (Fig. 5). The model also suggests that after approximately 20 weeks, the ZIKV epidemic will be over, even if no prevention program is implemented. Since our model does not include demographic birth-death and the disease death terms, the final outbreak size can be calculated by integrating the term $\beta_h S_h(t) I_m(t)$ from the beginning of infection to the time when epidemic ends. We found that the final size of the epidemic can reach nearly 100% without prevention indicating that almost the entire population can be infected with ZIKV during the epidemic period.

Effect of prevention programs on disease outcomes. We evaluated two illustrative prevention programs: one that reduces contact between mosquito and human, and another that decreases the mosquito lifespan. Reducing the contact between mosquito and human refers to a variety of programs, including utilization of the mosquito nets, wearing skin-covering clothes, and using mosquito repellents. Similarly, decreasing the mosquito lifespan refers to the program such as use of insecticides or other chemicals which aim to inhibit mosquito population growth.

If ϕ with $0 \leq \phi \leq 1$ is an effectiveness of the first prevention program (i.e. the reduction of contact between human and mosquito), implementing such programs causes the following

transformation of our model: $\hat{\beta}_h \longrightarrow (1-\phi)\hat{\beta}_h$ and $\beta_m \longrightarrow (1-\phi)\beta_m$. Our model suggests that reducing mosquito and human contact by at least 60% (i.e., when $\phi \geq 0.6$) would decrease the prevalence of ZIKV to almost negligible level (Fig. 6). In this case, the final outbreak size reduces dramatically from 100% to nearly 10%.

Similarly, a decrease in mosquito lifespan (the second prevention program) with effectiveness θ, i.e., the reduction of mosquito lifespan by θ times, changes our model causing $\lambda_m \rightarrow \theta\lambda_m$. With such prevention programs, the prevalence of ZIKV decreases to negligible level when mosquito death is increased by at least a factor of three, i.e., $\theta \geq 3$ (Fig. 7). Also, this prevention effort can reduce the final outbreak size from about 100% to nearly 10%.

Discussion

In this study, we formulated the mathematical models of between-hosts transmission dynamics of ZIKV infection, thoroughly investigated the fitting procedure, and analyzed the parameters that can be estimated from a given limited data. In addtion, we used the recently expanded *complex-step* method to calculate sensitivities and related confidence intervals of estimated parameters. Using the properly estimated parameters, we computed the basic reproduction number and performed extensive analysis and simulation of the models to investigate the short-term and long-term dynamics of the disease, prevalence of infections, and effect of prevention programs on disease outcomes.

While previous studies[21] used some of these island data to estimate six parameters, our results strongly suggest that these data sets do not contain sufficient information to estimate more than three parameters in islands of French Polynesia and more than two parameters in Yap island. Our analysis also showed that the parameters that can be estimated may vary from Island to Island, suggesting that the same paramters can not be estimated from each island and the parameters estimated using the standard techniques across all islands may provide misinformation about the ZIKV transmission dynamics. Identifiction of paramters that can be estimated as we obtained in this study can provide more robust parameters related to ZIKV transmission dynamics.

Applying our model, we predicted that a small portion of infections were reported (2.85 % - 20.59 %) as suspected cases across the island (Table 2). This does not necessarily indicate that the non-reported cases were asymptomatic; rather the individuals may have had mild symptoms and hence did not enter the healthcare system. This phenomenon was supported by the household survey following the Yap island outbreak in 2007[9].

Our estimated basic reproduction number, R_0, from best fitted model varied reasonably from island to island (Table 3). The R_0 value reflects that the ZIKV spread rapidly through the islands. This is reasonable since the people and mosquitos generally live in close community in an island life and may interact with each other with the ZIKV symptoms. Based on sensitivity analysis on basic reproduction number, we found that the value of R_0 is highly dependent on the mosquito life span. By lowering this value or in other words controlling mosquito growth, R_0 can significantly be reduced and thus an epidemic can be avoided.

Our detailed investigation on prevalence and infection provided some valuable conclusion. The prevalence started to increase at the beginning and reached to its peak in between 8 to 10 weeks of the outbreak (Fig. 5). Then, it gradually started to decrease since more humans were recovering from the virus than those with the new ZIKV infections. Since mosquito bite is the main reason of disease propagation, our result showed that reducing the human and mosquito contact could create a safe environment. Our study found that almost 100% of the island people were infected during the outbreak and the results is consistent with the other studies[21]. Our study

also showed that reducing the contact about 60% between human and mosquito can drastically reduce both peak prevalence and final outbreak size and almost eradicate the ZIKV infection (Fig. 6). The outcome is almost identical for reducing the mosquito lifespan (Fig. 7). The disease can completely be exterminated by lowering the mosquito lifespan by a factor of 3 to 4 times its base span.

The potential limitation of our model is that we modeled on island population who may have close proximity to one another at all times. Consequently, our results may not be generalizable to other populations. However, our results are relevant for many settings that share characteristics of our population including military units, college campus, nursing homes, boarding schools, and other rural communities, in which the community is surrounded by a large region with low population, approximating a closed population. Secondly, we did not consider the seasonal variation in transmission as a result of climate factors in our analysis since the outbreaks ended before there was a substantial seasonal change in rainfall or temperature. Such changes could influence the extrinsic incubation period and mortality of mosquitoes, and hence disease transmission. If the outbreaks had ended as a result of seasonality, rather than depletion of susceptible populations, it would reduce the estimated proportion of the infected population.

The main goals of this effort were to gain deeper insight into the mechanisms of epidemilogical spread of ZIKV infection and to evaluate aproprite prevention startegies. The results identified the importance of properly estimating the ZIKV infection related parameters from the given survey data. In conclusion, this work offered novel insight into ZIKV related parameters and ZIKV infection dynamics, and presented details about the short-term and long-term dynamics of the disease, prevalence of infections, and effect of prevention programs on disease outcomes.

Materials and methods

Experimental data. In this study, we utilized the data containing number of suspected ZIKV infections from six main regions (Tahiti, Iles sous-le-vent, Moorea, Tuamotu-Gambier, Marquises, and Australes) of French Polynesia, reported weekly between October 2013 and March 2014 [25], and one region of the Federated States of Micronesia (Yap Island), reported weekly between April 2007 and July 2007 [9]. In the ZIKV outbreak data of French Polynesia, clinical cases were defined as suspected cases if they were presented to health practitioners with rash and/or mild fever and at least two of the following signs: conjunctivitis, arthralgia, and edema. In total, 8,744 suspected cases were reported from the health sentinel sites. Similarly, in the Yap Island data, researchers reviewed medical records and conducted prospective surveillance at the hospital and all four health centers on Yap to identify patients with suspected ZIKV disease[9]. Suspected cases had the following characteristics: acute onset of generalized macular or popular rash, arthritis or arthralgia, or nonpurulent conjunctivitis. Out of the total 1,276 households tested on Yap Island, 185 cases were identified as suspected ZIKV disease, which we extrapolated for whole population of Yap Island. We obtained population data for these Islands from the 2012 French Polynesia Census [26] and the Federated States of Micronesia 2000 Census [27].

Mathematical Model. We developed a compartmental mathematical model to describe the ZIKV transmission dynamics, similar to the ones previously used for vector-borne transmission[28,29]. The humans were modeled using a susceptible-exposed-infectious-recovered (SEIR) framework, whereas the mosquitos were modeled as susceptible-exposed-infectious (SIE) framework (Fig. 8).

In this model, exposed classes were incorporated to include delays as a result of intrinsic (human) and extrinsic (mosquito) incubation periods.

In the model system, S_h represents the number of susceptible humans, E_h is the number of humans currently in their incubation period, I_h is the number of infectious humans, and R_h is the number of humans that have recovered from the ZIKV infection. Similarly, S_m, E_m , and I_m represent the susceptible, exposed, and infectious mosquitos, respectively. The dynamics of our ZIKV epidemiological model are governed by the following system:

$$\left.\begin{aligned} \frac{dS_h}{dt} &= -\beta_h S_h I_m \\ \frac{dE_h}{dt} &= \beta_h S_h I_m - \alpha_h E_h \\ \frac{dI_h}{dt} &= \alpha_h E_h - \gamma_h I_h \\ \frac{dR_h}{dt} &= \gamma_h I_h \end{aligned}\right\} \tag{3}$$

$$\left.\begin{aligned} \frac{dS_m}{dt} &= \lambda_m N_m - \frac{\beta_m S_m I_h}{N_h} - \lambda_m S_m \\ \frac{dE_m}{dt} &= \frac{\beta_m S_m I_h}{N_h} - (\lambda_m + \alpha_m) E_m \\ \frac{dI_m}{dt} &= \alpha_m E_m - \lambda_m I_m \end{aligned}\right\} \tag{4}$$

where $N_h = S_h + E_h + I_h + R_h$ represents the total number of the humans and $N_m = S_m + E_m + I_m$ represents the total number of mosquitos. The parameters $1/\alpha_h$ represents the human incubation period, $1/\alpha_m$ is the mosquito incubation period, $1/\gamma_h$ represents the human infectious period, and $1/\lambda_m$ is the mosquito life-span. In this model, susceptible humans get infected through the bites by infected mosquitos at a mosquito-to-human transmission rate β_h and a susceptible mosquito get infected when it bites infected humans at the human-to-mosquito transmission rate β_m.

Since the death due to ZIKV was not reported during the period of epidemics, we have ignored disease death rate terms in the model. We also consider a closed population (i.e. a population with no births, deaths or continual immigration), since the mean human lifespan is much longer than the outbreak duration, and entry and exit of people inside the island are negligible during this short period of outbreak. We assumed all people transmitted at the same rate, regardless of whether they displayed symptoms or were reported as cases. We considered that no transmission typically occurs before the exposed individuals enter the infectious class.

We introduced variables $s_h = S_h/N_h$, $e_h = E_h/N_h$, $i_h = I_h/N_h$, $r_h = R_h/N_h$, $s_m = S_m/N_m$, $e_m = E_m/N_m$, and $i_m = I_m/N_m$, scaled to their corresponding total population size. This allows the standard simplification of $r_h = 1 - s_h - e_h - i_h$ and $s_m = 1 - e_m - i_m$, thereby reducing the population-wide ZIKV model to the following five dimensional system:

$$\frac{ds_h}{dt} = -\hat{\beta}_h s_h i_m$$
$$\frac{de_h}{dt} = \hat{\beta}_h s_h i_m - \alpha_h e_h$$
$$\frac{di_h}{dt} = \alpha_h e_h - \gamma_h i_h \quad (5)$$
$$\frac{de_m}{dt} = \beta_m i_h (1 - e_m - i_m) - (\lambda_m + \alpha_m) e_m$$
$$\frac{di_m}{dt} = \alpha_m e_m - \lambda_m i_m$$

where $\hat{\beta}_h = \beta_h N_m$.

Parameter estimation. Serological analysis of samples from blood donors between July 2011 and October 2013 suggested that only 0.8% of the population of French Polynesia were seropositive to ZIKV [30]; we therefore assumed that the population was fully susceptible initially. The mosquito incubation period and the mosquito lifespan were previously estimated to be 10 days [31,32] and 15 days [32,33], respectively. Therefore, we took constant values of $1/\alpha_m$ = 10 days and $1/\lambda_m$ = 15 days for all islands. We also assumed that the outbreak began with one initial exposed and one infectious human (i.e., $e_h(0) = i_h(0) = 1/N_H$), and one exposed and one infectious mosquito (i.e., $e_m(0) = i_m(0) = 0.005$). With these parameters and initial conditions fixed, the remaining five parameters, α_h ,γ_h, $\hat{\beta}_h$, $\beta_m$and η**,** where η is the proportion of case reported, were estimated using a complete data-fitting procedure combined with detailed confidence interval analysis as discussed below. Description of the parameters, and their fixed values are given in Table 4.

Model fitting to the data. We fitted the model to cumulative weekly new infection data. The cumulative new infections predicted by our model, $P(t)$, are given by the solution of the following equation:

$$\frac{dP}{dt} = \eta \alpha_h e_h N_h \quad (6)$$

We solved the system of differential equations numerically using a fourth order Runge–Kutta method and used the solutions to obtain the best-fit parameters via a nonlinear least squares regression method that minimizes the following sum of the squared residuals.

$$J(\Phi) = \sum_{k=1}^{n} [\, P_{t_k}(\Phi) - \bar{P}_{t_k}]^2 \qquad (7)$$

where $\Phi = (\Phi_1,\ \Phi_2, \Phi_3, \Phi_4, \Phi_5) = (\hat{\beta}_h\ ,\ \beta_m, \alpha_h, \gamma_h, \eta\ )$; P_{t_k} and $\bar{P}_{t_k}$ are cumulative infected population values predicted by the model and those obtained from the survey data, respectively. Here, n represents the total number of data points available for the model fitting. All computations were carried out in MATLAB (The MathWorks, Inc., Natick, MA).

Computaion of confidence intervals. To obtain confidence limits for the estimated parameters, we computed standard errors for Φ by using similar ideas as described in Banks, et al. [34]. For this, we first compute the sensitivity matrix Ψ of the parameters.

$$\Psi = \begin{bmatrix} \frac{\partial P_{t_1}}{\partial \Phi_1} & \frac{\partial P_{t_1}}{\partial \Phi_2} & \frac{\partial P_{t_1}}{\partial \Phi_3} & \frac{\partial P_{t_1}}{\partial \Phi_4} & \frac{\partial P_{t_1}}{\partial \Phi_5} \\ \frac{\partial P_{t_2}}{\partial \Phi_1} & \frac{\partial P_{t_2}}{\partial \Phi_2} & \frac{\partial P_{t_2}}{\partial \Phi_3} & \frac{\partial P_{t_2}}{\partial \Phi_4} & \frac{\partial P_{t_2}}{\partial \Phi_5} \\ \vdots & \vdots & \vdots & \vdots & \vdots \\ \frac{\partial P_{t_n}}{\partial \Phi_1} & \frac{\partial P_{t_n}}{\partial \Phi_2} & \frac{\partial P_{t_n}}{\partial \Phi_3} & \frac{\partial P_{t_n}}{\partial \Phi_4} & \frac{\partial P_{t_n}}{\partial \Phi_5} \end{bmatrix}.$$

Since we are unable to compute $\frac{\partial P_{t_k}}{\partial \Phi_j}$, $j = 1,2, \ldots .5$, and $k = 1, 2, \ldots \ldots n$ analytically from our model, we use the following *complex-step* approximation to compute the partial derivatives:

$$\frac{\partial P_{t_n}}{\partial \Phi_j} \approx D_h^j\left(P_{t_k}\right) = \frac{Im\,[P_{t_k}(\Phi_h + ih)]}{h}\ ,\ \ j = 1,2, \ldots 5, \text{ and } k = 1, 2, \ldots n$$

where *h* is taken to be a small positive constant (*h= 10 $^{-40}$* in our computations) and *i* is the unit imaginary number. With these, we compute an approximation to the sensitivity matrix Ψ denoted by $\widehat{\Psi}$. Then we take $\sqrt{(\sigma^2\ \{\widehat{\Psi}^T\widehat{\Psi}\}^{-1})_{ii}}$, where $\sigma^2 \approx \hat{\sigma}^2 = J(\Phi^*)/(n-5)$ and Φ^* are the basic estimated parameter values, to be the standard deviation for the parameter Φ_j, $j = 1,2 \ldots .5$. We also computed the standard errors using the usual forward finite difference method for comparison and validation. A brief derivation of the method is provided in supplementary materials and more detailed description can be found in Banks, et al. [35,36].

Data Availability: All data generated or analyzed during this study are included in this published article (and its Supplementary Information files).

References

1 Musso, D. *et al.* Potential sexual transmission of Zika virus. *Emerging infectious diseases* **21**, 359-361 (2015).

2 Gao, D. *et al.* Prevention and Control of Zika as a Mosquito-Borne and Sexually Transmitted Disease: A Mathematical Modeling Analysis. *Scientific Reports* **6**, 28070, doi:10.1038/srep28070 (2016).
3 D'Ortenzio, E. *et al.* Evidence of Sexual Transmission of Zika Virus. *The New England journal of medicine* **374**, 2195-2198 (2016).
4 Chouin-Carneiro, T. *et al.* Differential Susceptibilities of Aedes aegypti and Aedes albopictus from the Americas to Zika Virus. *PLoS neglected tropical diseases* **10**, e0004543, doi: 10.1371/journal.pntd.0004543 (2016).
5 Freire, C. C. d. M., Iamarino, A., Neto, D. F. d. L., Sall, A. A. & Zanotto, P. M. d. A. Spread of the pandemic Zika virus lineage is associated with NS1 codon usage adaptation in humans. *bioRxiv*, doi:10.1101/032839 (2015).
6 Grard, G. *et al.* Zika virus in Gabon (Central Africa)--2007: a new threat from Aedes albopictus, *PLoS neglected tropical diseases* **8**, e2681, doi:10.1371/journal.pntd.0002681 (2014).
7 (WHO), W. H. O. *WHO statement on the first meeting of the International Health Regulations (2005) Emergency Committee on Zika virus and observed increase in neurological disorders and neonatal malformations,February 1, 2016*, <http://www.who.int/mediacentre/news/statements/2016/1st-emergency-committee-zika/en/>
8 (CDC), C. f. D. C. a. P. *CDC Emergency Operations Center moves to highest level of activation for Zika response, Febraury 3, 2016*, <https://www.cdc.gov/media/releases/2016/s0208-zika-eoca-activation.html>
9 Duffy, M. R. *et al.* Zika virus outbreak on Yap Island, Federated States of Micronesia. *The New England journal of medicine* **360**, 2536-2543 (2009).
10 Oehler, E. *et al.* Increase in cases of Guillain-Barre syndrome during a Chikungunya outbreak, French Polynesia, 2014 to 2015. *Euro surveillance : bulletin Europeen sur les maladies transmissibles = European communicable disease bulletin* **20**, 30079, doi:10.2807/1560-7917.ES.2015.20.48.30079 (2015).
11 Oehler, E. *et al.* Zika virus infection complicated by Guillain-Barre syndrome--case report, French Polynesia, December 2013. *Euro surveillance : bulletin Europeen sur les maladies transmissibles = European communicable disease bulletin* **19** (2014).
12 Schuler-Faccini, L. *et al.* Possible Association Between Zika Virus Infection and Microcephaly - Brazil, 2015. *MMWR. Morbidity and mortality weekly report* **65**, 59-62 (2016).
13 Mlakar, J. *et al.* Zika Virus Associated with Microcephaly. *The New England journal of medicine* **374**, 951-958 (2016).
14 Mallela, A., Lenhart, S. & Vaidya, N. K. HIV–TB co-infection treatment: Modeling and optimal control theory perspectives. *Journal of Computational and Applied Mathematics* **307**, 143-161 (2016).
15 Mutua, J. M., Wang, F. B. & Vaidya, N. K. Modeling malaria and typhoid fever co-infection dynamics. *Mathematical biosciences* **264**, 128-144 (2015).
16 Keeling, M. J. & Rohani, P. *Modeling Infectious Diseases in Humans and Animals*. (Princeton University Press, 2011).
17 Anderson, R. M. & May, R. M. *Infectious Diseases of Humans: Dynamics and Control*. (OUP Oxford, 1992).

18 Vaidya, N. K. *et al.* Modelling the epidemic spread of an H1N1 influenza outbreak in a rural university town. *Epidemiology and infection* **143**, 1610-1620 (2015).
19 Akbari, S., Vaidya, N. K. & Wahl, L. M. The time distribution of sulfadoxine-pyrimethamine protection from malaria. *Bulletin of mathematical biology* **74**, 2733-2751 (2012).
20 Zhang, Q. *et al.* Projected spread of Zika virus in the Americas. *bioRxiv*, doi:https://doi.org/10.1101/066456 (2016).
21 Kucharski, A. J. *et al.* Transmission Dynamics of Zika Virus in Island Populations: A Modelling Analysis of the 2013-14 French Polynesia Outbreak. *PLoS neglected tropical diseases* **10**, e0004726, doi:10.1371/journal.pntd.0004726 (2016).
22 Lessler, J. *et al.* Times to Key Events in the Course of Zika Infection and their Implications for Surveillance: A Systematic Review and Pooled Analysis. *bioRxiv*, doi:https://doi.org/10.1101/041913 (2016).
23 Musso, H.-P. M. A.-L. V. D. Bilan de l'épidémie a virus ZIKA en Polynésie Francaise 2013–2014. . *Bulletin d'Information Sanitaires, Epidemiologiques et Statistiques* (2015).
24 van den Driessche, P. & Watmough, J. Reproduction numbers and sub-threshold endemic equilibria for compartmental models of disease transmission. *Mathematical biosciences* **180**, 29-48 (2002).
25 publique., C. d. h. e. d. s. *Surveillance de la dengue et du zika en Polynèsie française.*, <http://www.hygiene-publique.gov.pf/IMG/pdf/bulletin_dengue_28-03-14.pdf> (2014).
26 économiques, I. n. d. l. s. e. d. é. *Population des subdivisions administratives de Polynésie française*, <http://www.insee.fr/fr/> (2012).
27 Housing, F. C. o. P. a. *Yap State Census Report* <http://www.pacificweb.org/DOCS/fsm/Yap2000Census/2000%20Yap%20Census%20Report_Final.pdf> (2000).
28 Pandey, A., Mubayi, A. & Medlock, J. Comparing vector-host and SIR models for dengue transmission. *Mathematical biosciences* (2013).
29 Manore, C. A., Hickmann, K. S., Xu, S., Wearing, H. J. & Hyman, J. M. Comparing dengue and chikungunya emergence and endemic transmission in A. aegypti and A. albopictus. *Journal of theoretical biology* **356**, 174-191 (2014).
30 Aubry, M. *et al.* Seroprevalence of arboviruses among blood donors in French Polynesia, 2011-2013. *International journal of infectious diseases : IJID : official publication of the International Society for Infectious Diseases* **41**, 11-12 (2015).
31 Boorman, J. P. & Porterfield, J. S. A simple technique for infection of mosquitoes with viruses; transmission of Zika virus. *Transactions of the Royal Society of Tropical Medicine and Hygiene* **50**, 238-242 (1956).
32 Andraud, M., Hens, N., Marais, C. & Beutels, P. Dynamic epidemiological models for dengue transmission: a systematic review of structural approaches. *PloS one* **7**, e49085, doi:10.1371/journal.pone.0049085 (2012).
33 Chikaki, E. & Ishikawa, H. A dengue transmission model in Thailand considering sequential infections with all four serotypes. *Journal of infection in developing countries* **3**, 711-722 (2009).
34 Banks, H. T., Hu, S. & Thompson, W. C. *Modeling and Inverse Problems in the Presence of Uncertainty*. (Taylor & Francis, 2014).

35 Banks, H. T., Bekele-Maxwell, K., Bociu, L., Noorman, M. & Tillman, K. The complex-step method for sensitivity analysis of non-smooth problems arising in biology. *Eurasian journal of Mathematical and Computer Applications* **3**, 15-68 (2015).
36 Banks, H. T., Bekele-Maxwell, K., Bociu, L. & Wang, C. Sensitivity via the complex-step method for delay di erential equations with non-smooth initial data. *Quarterly of Applied Mathematics* **75**, 231-248 (2017).

Acknowledgements

This research was supported in part by the National Institute on Alcohol Abuse and Alcoholism under grant number 1R01AA022714-01A1, and in part by the Air Force Office of Scientific Research under grant number AFOSR FA9550-15-1-0298.

Author Contributions

M.R., L.C., and N.V. developed the model structure; M.R. and N.V. performed the modeling and numerical analysis; M.R., N.V., K.B.M, and H.T.B. performed data and statistical analysis; All authors discussed the results and contributed to the writing of the manuscript.

Additional Information

Competing financial interests: The authors declare no competing financial interest.

List of tables

Parameter	Tahiti	Sous-le-vent	Moorea	Tuamotu-Gambier	Marquises	Australes	Yap
$\hat{\beta}_h$	1.5547	0.8794	0.9569	0.9751	0.4601	1.7768	0.1787
S.Error(cs)	0.9818	0.5866	0.5296	2.2552	0.5255	3.4539	3.0457
S.Error(fd)	0.9866	0.5760	0.5327	2.2556	0.5256	3.5184	3.0622
β_m	0.0561	0.0685	0.1105	0.0771	0.1957	0.0319	1.2873
S.Error(cs)	0.0996	0.0468	0.1887	0.3168	0.4066	0.0944	8.9866
S.Error(fd)	0.0997	0.0463	0.1899	0.3164	0.4068	0.0960	9.1026
$1/\alpha_h$	12.0048	8.2576	11.4286	12.0048	4.0000	12.0048	8.7873
S.Error(cs)	4.8577	4.4678	3.7759	9.0437	3.1235	8.7855	8.4518
S.Error(fd)	4.8819	4.4281	3.789	9.0449	3.1237	8.8293	8.4538
$1/\gamma_h$	12.0048	12.0048	12.0048	8.0064	4.0000	11.3766	12.0048
S.Error(cs)	8.9100	5.1579	8.7961	6.5544	2.8517	8.9943	10.8230
S.Error(fd)	8.9180	5.1376	8.8119	6.5524	2.8517	9.0265	10.8501
η x 100	2.8400	3.9400	2.8500	3.9900	5.9600	11.5800	20.0400
S.Error(cs)	0.0142	0.0589	0.0135	0.3638	0.5664	0.6336	4.7154
S.Error(fd)	0.0142	0.0581	0.0135	0.3636	0.5678	0.6444	4.7561

Table 1. Parameters obtained from fitting the model to data with all five parameters estimated.

Parameter	Tahiti	S-L-V	Moorea	T-G	Marquises	Australes	Yap
$\widehat{\boldsymbol{\beta}}_{\boldsymbol{h}}$ *[95% CI]*	0.9510 [fixed]	0.9510 [fixed]	0.9510 [fixed]	0.9510 [fixed]	0.9510 [fixed]	0.9510 [fixed]	0.9056 [0.7898 1.0214]
$\boldsymbol{\beta_m}$ *[95% CI]*	0.0622 [0.0537 0.0707]	0.0498 [0.0367 0.0629]	0.1159 [0.0761 0.1557]	0.0586 [0.0499 0.0673]	0.0352 [0.0202 0.0502]	0.0489 [0.0417 0.0561]	0.0654 [fixed]
$\boldsymbol{1/\alpha_h}$ *[95% CI]*	4.000 [2.8680 5.1320]	6.0015 [fixed]	11.4286 [8.2931 14.5641]	10.2881 [8.4708 12.1054]	6.0015 [fixed]	4.0000 [2.7576 5.2424]	6.0015 [fixed]
$\boldsymbol{1/\gamma_h}$ *[95% CI]*	11.0865 [fixed]	12.0048 [7.0885 16.9211]	11.0865 [fixed]	11.0865 [fixed]	12.0048 [5.1039 18.9057]	11.0865 [fixed]	11.0865 [fixed]
η x 100 *[95% CI]*	2.8500 [2.8212 2.8788]	3.9800 [3.9078 4.0522]	2.8500 [2.8266 2.8734]	3.9800 [3.9340 4.0260]	5.8400 [5.4251 6.2549]	11.6100 [11.2970 11.9230]	20.5900 [18.6921 22.4879]

Table 2. Best parameters estimated with reliable confidence intervals.

Basic Reproduction Number	Tahiti	Sous-le-vent	Moorea	Tuamotu-Gambier	Marquises	Australes	Yap
R_0	2.4294	2.2621	3.3163	2.3581	1.9018	2.1541	2.4309

Table 3. Basic Reproduction number (R_0) for individual Islands.

Parameter	Description	Value
$1/\alpha_m$	Mosquito incubation period	10 days (Fixed)
$1/\lambda_m$	Mosquito life-span	15 days (Fixed)
$1/\alpha_h$	Human incubation period	Data fitting
$1/\gamma_h$	Human infectious period	Data fitting
$\hat{\beta}_h$	Mosquito-to-human transmission rate	Data fitting
β_m	Human-to-mosquito transmission rate	Data fitting
η	Proportion of case reported	Data fitting

Table 4. Parameter description and values.

List of figures

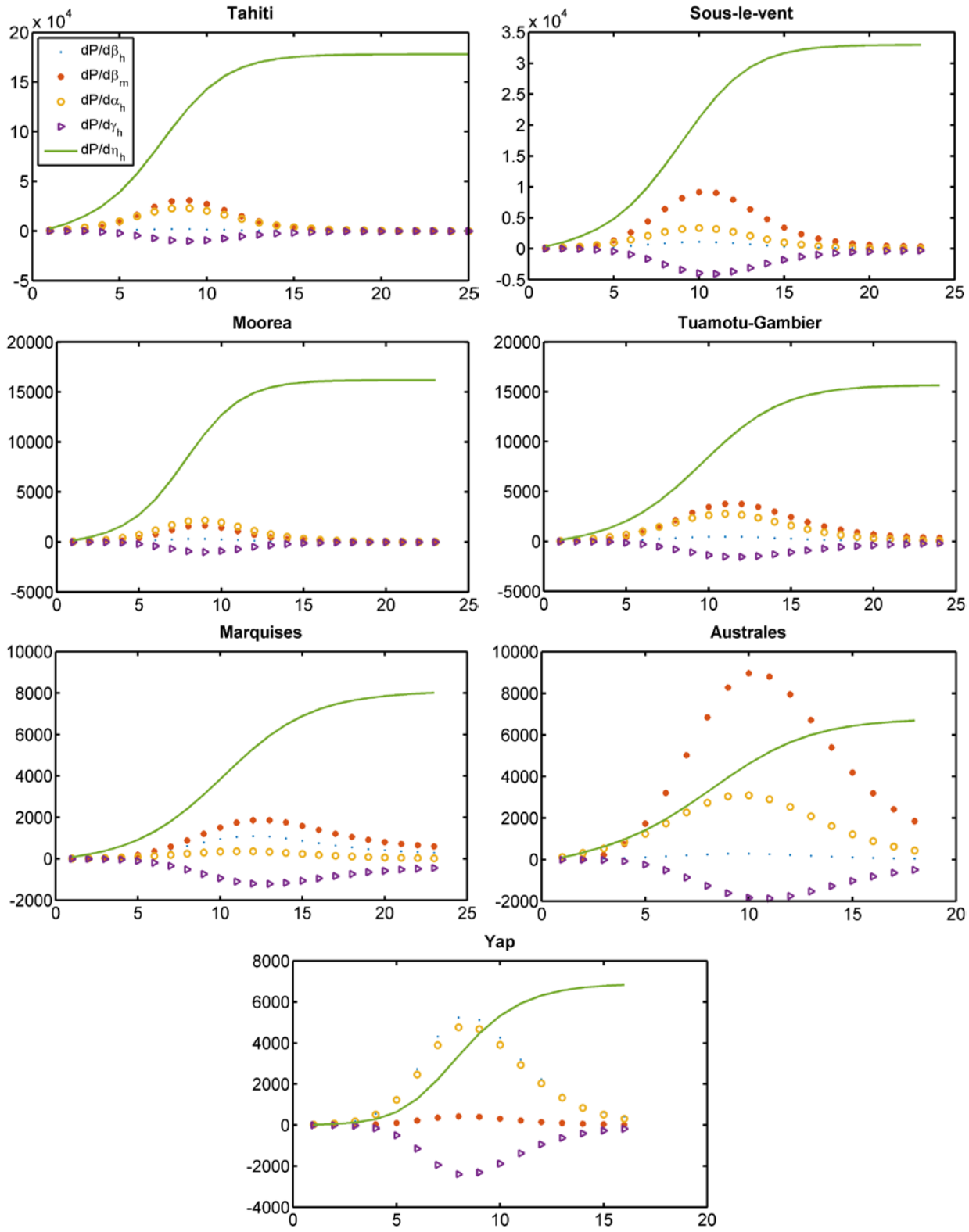

Figure 1. Sensitivity graphs of P to $\hat{\beta}_h$, $\beta_m, \alpha_h, \gamma_h,$ and η at estimated values.

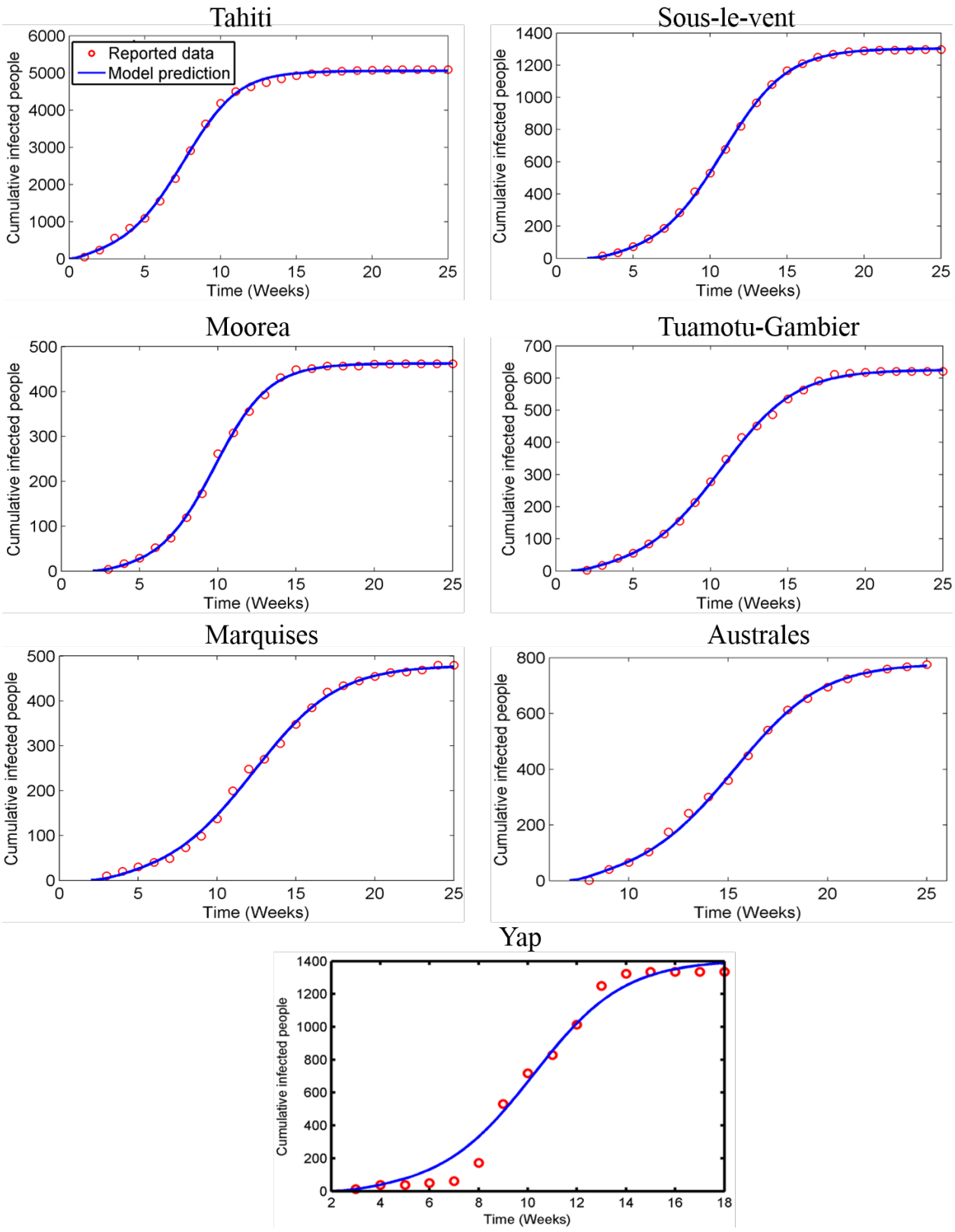

Figure 2. Data fitting for each individual island for weekly cumulative infected humans.

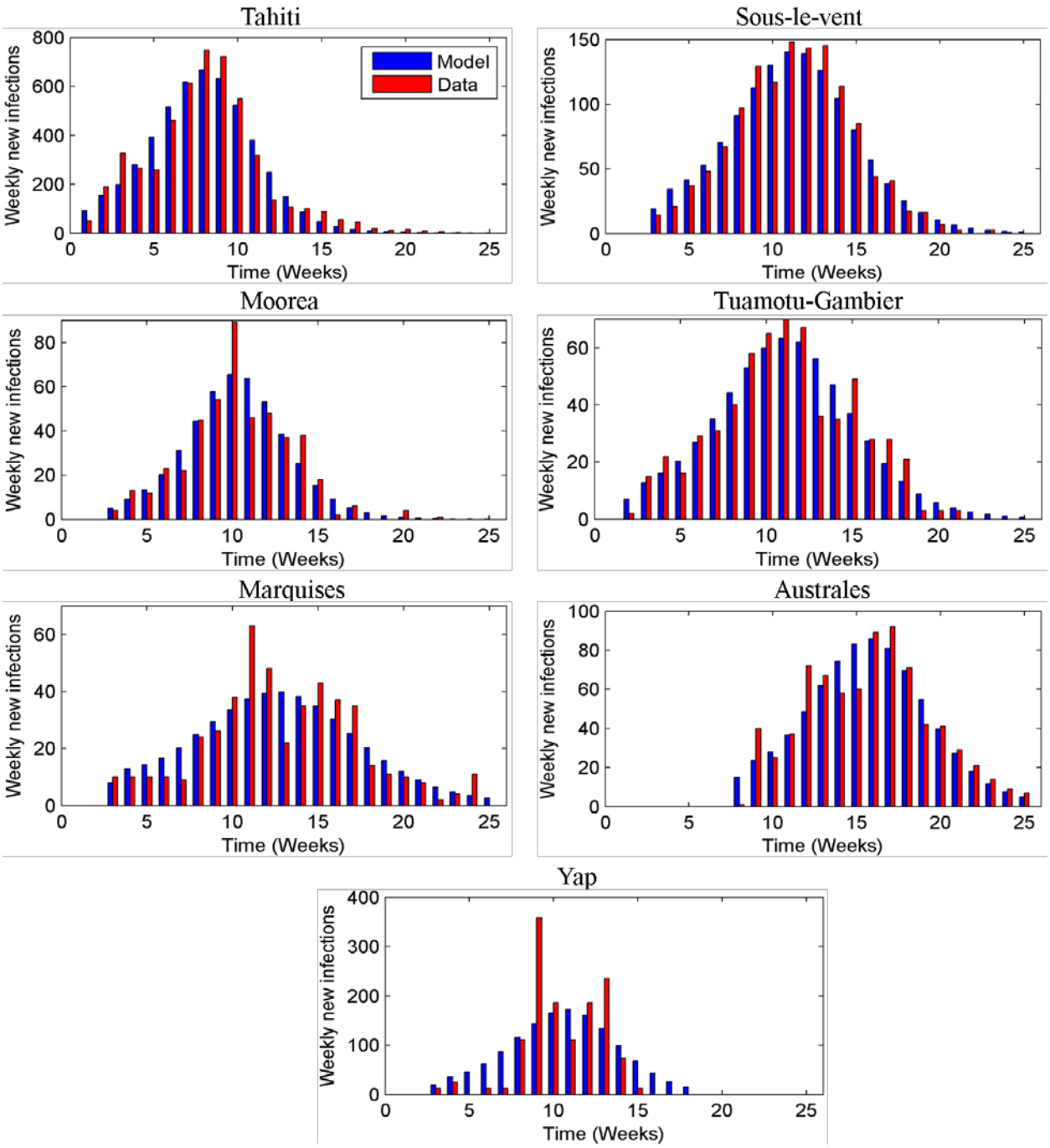

Figure 3. Comparison between experimental data and model prediction for weekly new infections.

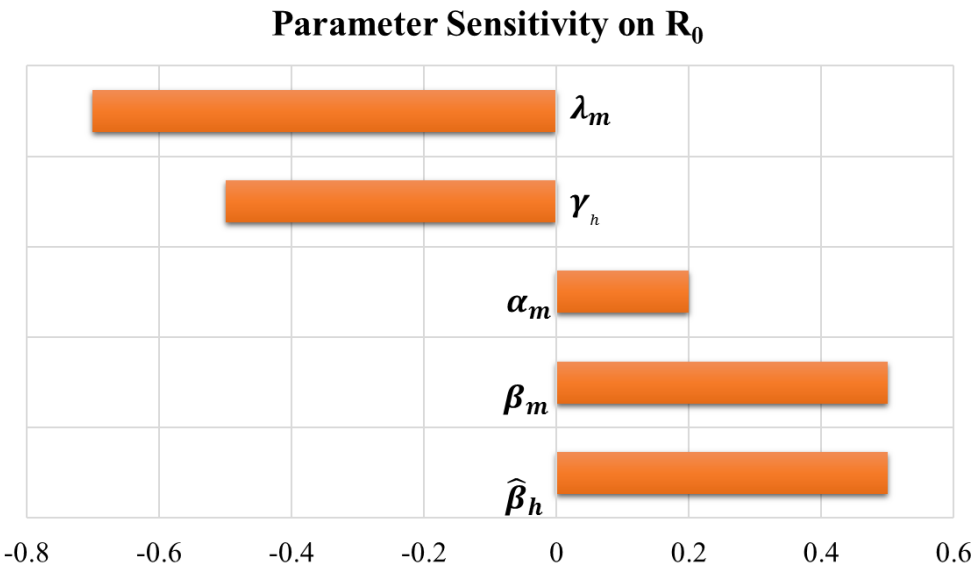

Figure 4. Sensitivity of parameters in the basic reproduction number.

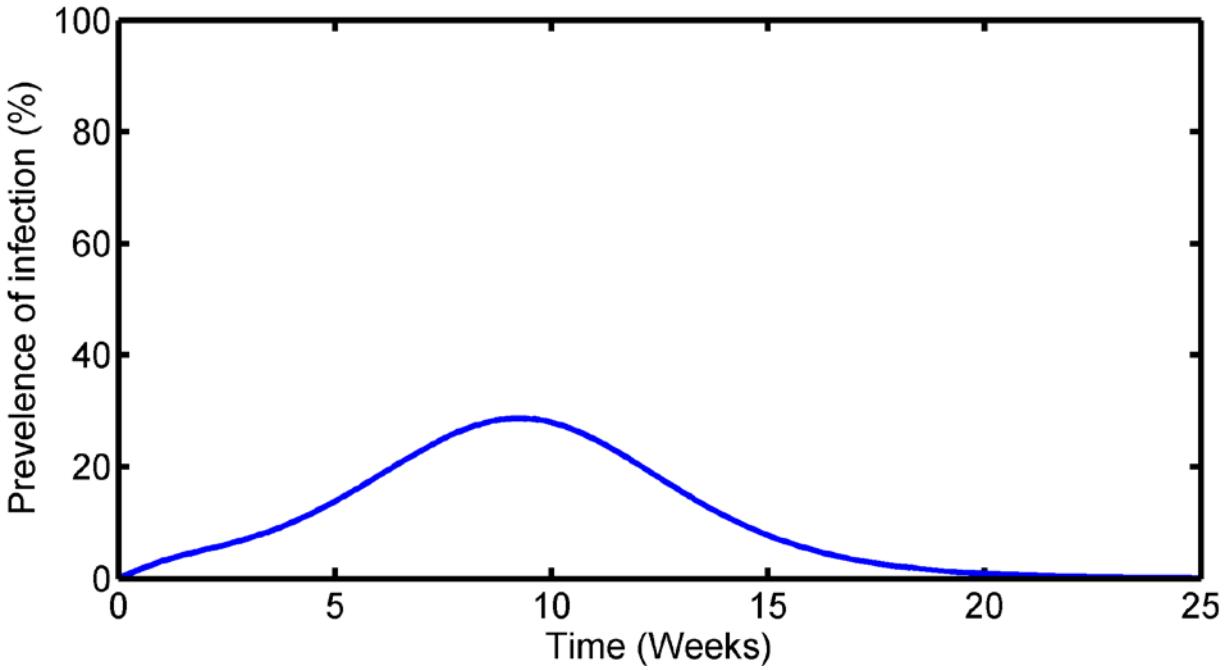

Figure 5. Mean prevalence of infection during a ZIKV epidemic.

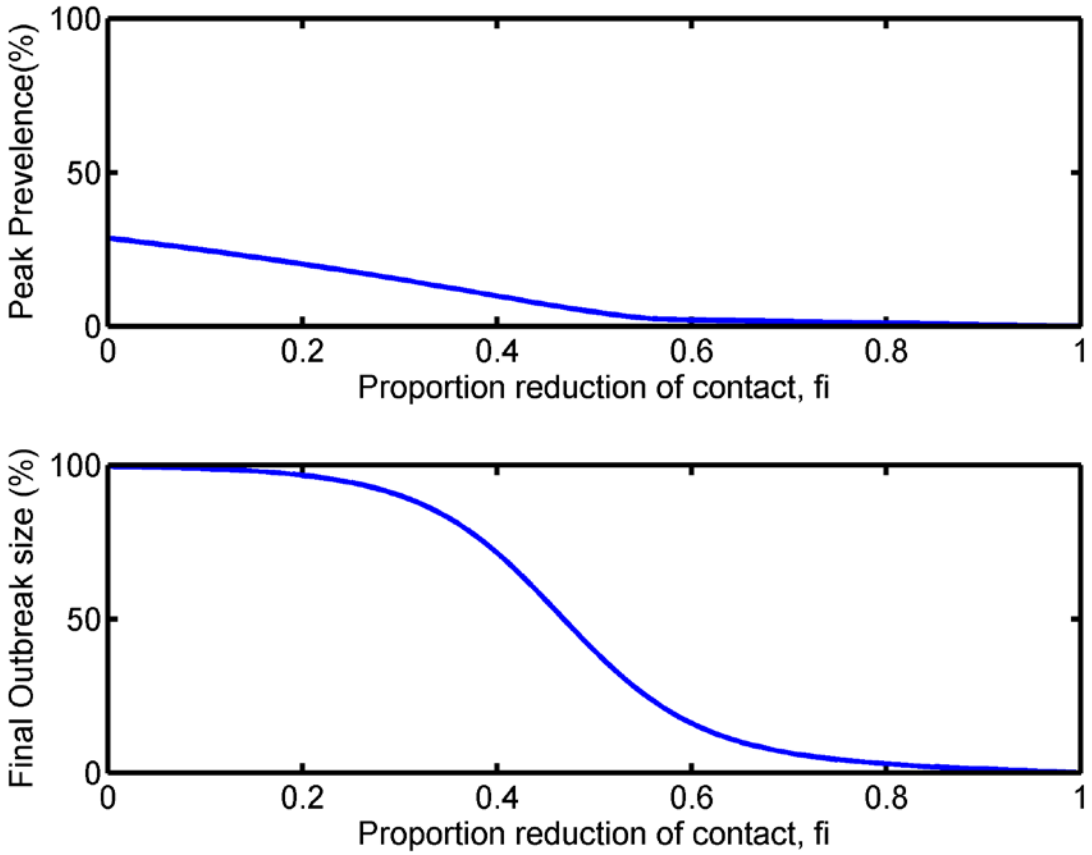

Figure 6. Peak prevalence during an epidemic and final outbreak size predicted by the mode for the prevention programs focused on reducing contact between humans and mosquitos.

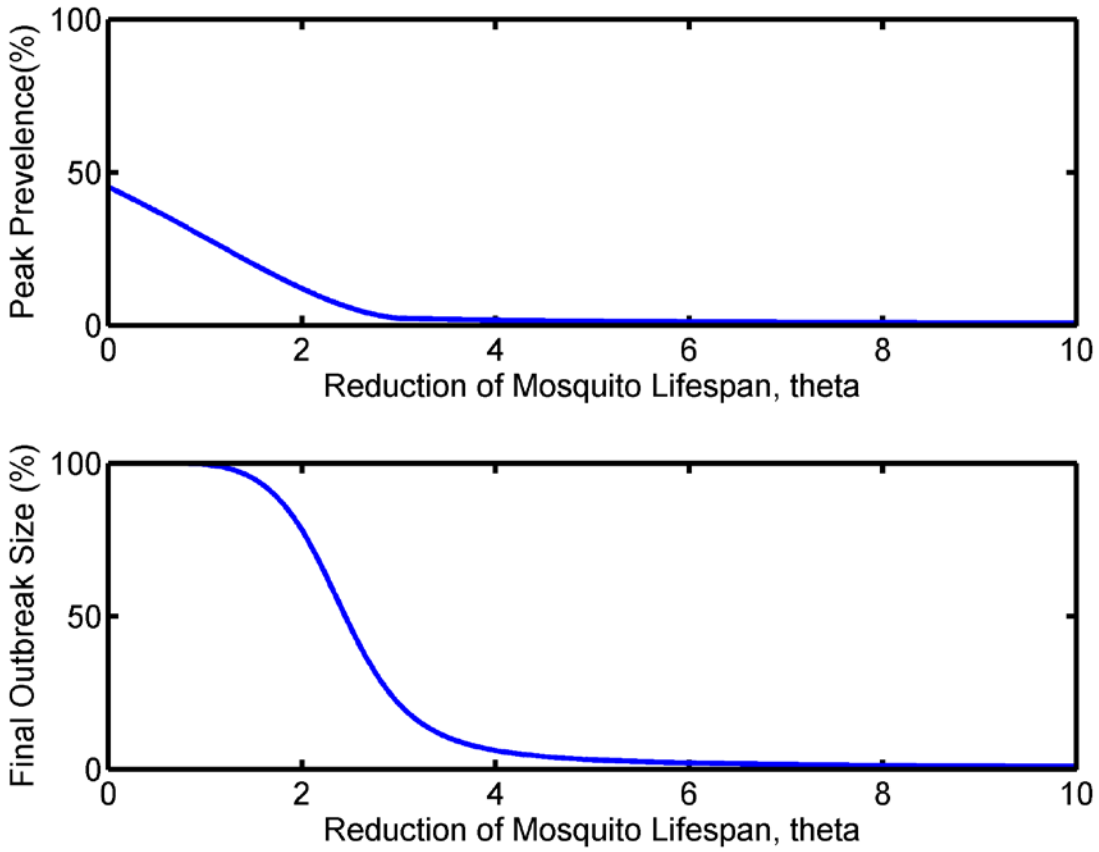

Figure 7. Peak prevalence during an epidemic and final outbreak size predicted by the mode for the prevention programs focused on reducing mosquito lifespan.

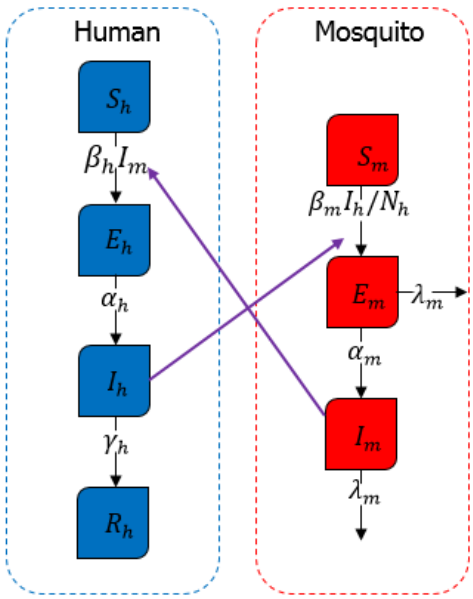

Figure 8. Schematic representation of human-vector transmission.

Supplemental Information: Complex-step method

Let $z = x + iy, x, y \in \mathbb{R}$ be a complex number and $f(z) = f(x, y) = r(x, y) + iv(x, y)$ be a function of a complex variable. If *f* is analytic, we have the following Cauchy-Riemann equations that establish the relationship between the real and imaginary parts of the function.

$$\frac{\partial r}{\partial x}(x, y) = \frac{\partial v}{\partial y}(x, y)\ ,\ \ \frac{\partial r}{\partial y}(x, y) = -\frac{\partial v}{\partial x}(x, y) \tag{S-1}$$

For a given step size h we can derive a finite difference-like first derivative estimate for real functions using complex calculus. From the first equation in (S-1), and the definition of derivatives we have

$$\frac{\partial r}{\partial x}(x, y) = \lim_{h \to 0} \frac{v(x, y + h) - v(x, y)}{h} \tag{S-2}$$

$$= \lim_{h \to 0} \frac{Im[f(x + i(y + h))] - Im[f(x + iy)]}{h} \tag{S-3}$$

If *f* takes a real-valued input, then $y = 0, f(x = r(x, 0)$, and $v(x, 0) = Im[f(x)] = 0$, Thus (S-2) becomes

$$\frac{\partial f}{\partial x} = \lim_{h \to 0} \frac{Im[f(x + ih)]}{h} \tag{S-4}$$

Therefore, for small *h*, we have the *complex-step* derivative approximation

$$\frac{\partial f}{\partial x} \approx \frac{Im[f(x + ih)]}{h} \tag{S-5}$$

This formula can also be obtained by approximating a C^2 function *f(q)* with a complex variable using a 2nd order *Taylor* expansion with remainder:

$$f\ (q + ih) \approx\ f(q) + ih\ f^{'}(q) + R(q)$$

where $R(q)$ is $O(h^2)$. Taking the imaginary parts of both sides and dividing by h gives

$$f^{'}(q) \approx\ \frac{Im[f(q+ih)]}{h} + O(h^2).$$

Terms of order h^2 and higher can be ignored because the step size *h* can be chosen up to machine precision. Thus the *complex-step* derivative is given by (S-5) with a truncation error $E_t(h) = \frac{h^2}{6} f^{(3)}(q)$. The method is accurate down to a specific step size we call h_{crit}. Below h_{crit}, underflow occurs and the approximation becomes useless.

The derivative estimate (S-5) constitutes a big advantage over the finite-difference approach. First, it is applicable for problems with less smoothness than analyticity (e.g., only C^2 functions of the parameters -see [35,36]. Moreover, the finite-difference approximation is subject to *subtractive error* due to the differencing operation. On the other hand, the accuracy of the complex-step estimates is only limited by the numerical precision of the algorithm that evaluates the function *f*. For detailed explanation, remarks on implementation procedures, we refer the reader to [35,36] and the references therein.

List of Tables

Parameter	Tahiti	S-L-V	Moorea	T-G	Marquises	Australes	Yap
$\hat{\beta}_h$	fixed (1)	fixed (1)	fixed (1)	fixed (1)	0.7976	fixed (1)	0.7763
S.Error					0.2331		1.5617
β_m	0.0557	0.0675	0.108	0.0682	0.1498	0.0898	fixed
S.Error	0.0318	0.0119	0.0331	0.0324	0.3015	0.0969	(0.1)
$1/\alpha_h$	4.1152	10.6952	12.0048	12.0048	fixed (12)	5.1467	7.9872
S.Error	1.2709	0.8397	1.5778	1.9283		1.5758	6.5531
$1/\gamma_h$	12.0048	12.0048	12.0048	9.1241	4.0000	4.3122	12.0000
S.Error	5.3508	2.1810	3.9437	3.2069	2.6637	2.3475	5.3238
η *x 100*	2.8500	3.9300	2.8500	3.9900	5.6900	12.0800	20.1900
S.Error	0.0227	0.0103	0.0132	0.0309	0.1814	0.3182	0.9149

Table S-1. Estimate of four parameters.

Parameter	Tahiti	S-L-V	Moorea	T-G	Marquises	Australes	Yap
$\hat{\beta}_h$	fixed (1)	fixed (1)	fixed (1)	fixed (1)	fixed (1)	fixed (1)	0.7763
S.Error							1.4958
β_m	0.0557	0.0812	0.1079	0.0547	0.0494	0.0432	fixed
S.Error	0.0037	0.0068	0.0177	0.0042	0.0099	0.0028	(0.1)
$1/\alpha_h$	4.1152	fixed (12)	11.9904	11.0988	fixed (12)	4.0000	7.9872
S.Error	0.5526		1.5129	0.9505		0.5392	6.4857
$1/\gamma_h$	fixed	10.2987	fixed (12)	fixed	12.0048	fixed (12)	fixed (12)
S.Error	(12)	1.3868		(12)	3.2302		
η *x 100*	2.8500	3.9400	2.8500	3.9700	5.6000	11.6200	20.1900
S.Error	0.0137	0.0099	0.0116	0.0207	0.0767	0.1359	0.7664

Table S-2. Estimate of three parameters.

Parameter	Tahiti	S-L-V	Moorea	T-G	Marquises	Australes	Yap
$\hat{\beta}_h$	fixed (1)	fixed (1)	fixed (1)	fixed (1)	fixed (1)	fixed (1)	0.9510
S.Error							0.0517
β_m	0.1252	0.0812	fixed	0.0585	fixed (0.1)	0.0916	fixed
S.Error	0.0040	0.0020	(0.1)	0.0008		0.0051	(0.1)
$1/\alpha_h$	fixed	fixed (12)	11.1982	fixed	fixed (12)	fixed (12)	fixed (12)
S.Error	(12)		0.1722	(12)			
$1/\gamma_h$	fixed	fixed (12)	fixed (12)	fixed	12.0048	fixed (12)	fixed (12)
S.Error	(12)			(12)	0.1478		
η *x 100*	2.8300	3.9400	2.8500	3.9700	5.8000	11.2100	20.4100
S.Error	0.0164	0.0245	0.0105	0.0175	0.0843	0.1843	0.6357

Table S-3. Estimate of two parameters.

List of figures

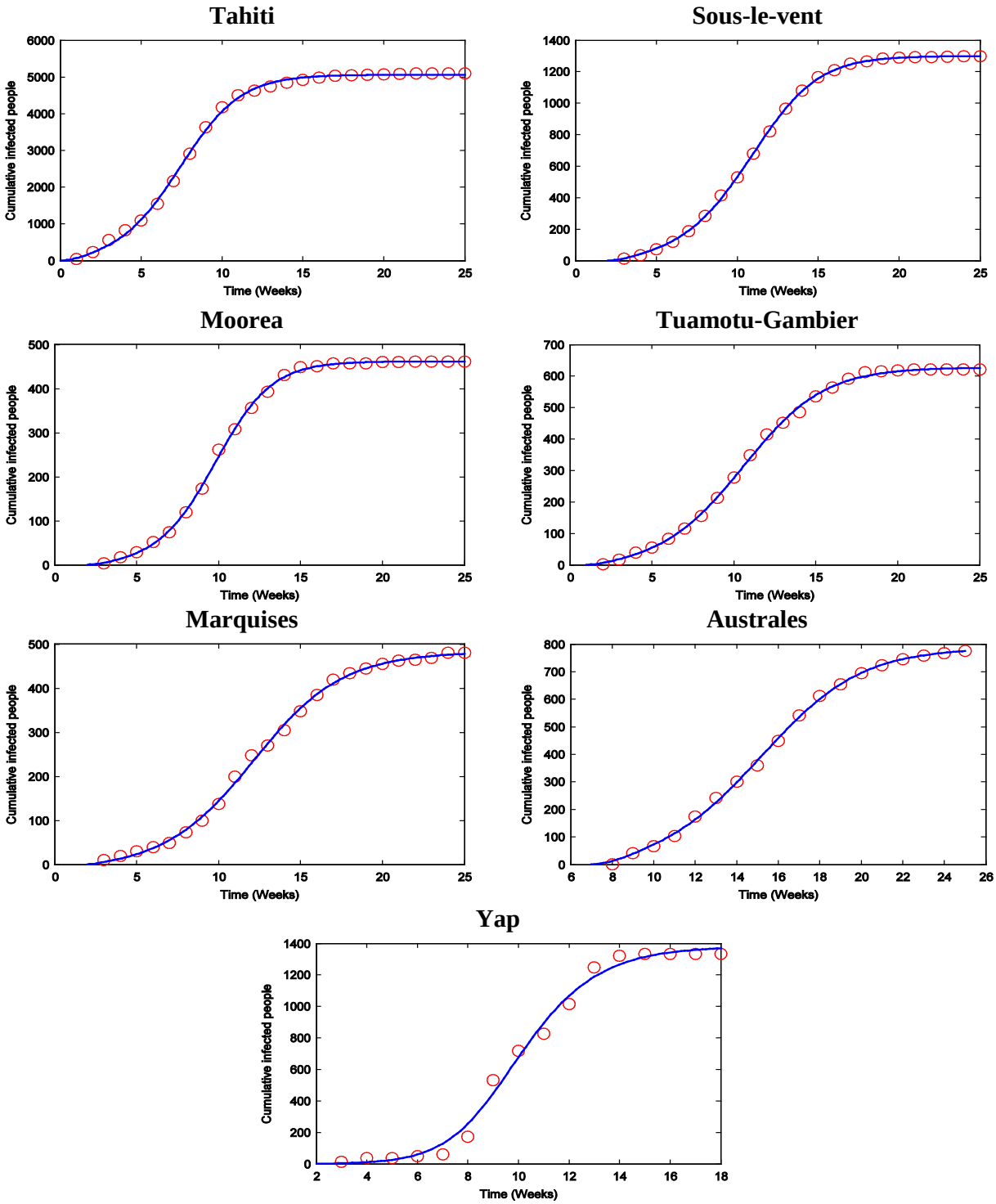

Figure S-1. Results of data fitting for each individual island. Red circle shows the weekly reported cumulative ZIKV cases from sentinel sites, and the solid blue line shows the model fits-to-data.